Gravitational Waves as a Probe of Origin of the Primordial Black Holes

Indra Kumar Banerjee and Ujjal Kumar Dey
Department of Physical Sciences, Indian Institute of Science Education and Research Berhampur, Transit Campus, Government ITI, Berhampur 760010, Odisha, India

Abstract

We consider the cumulative stochastic gravitational wave background as a method to extract information regarding the origin of primordial black holes. For this, we consider a mechanism such as the first order phase transition, which can create stochastic gravitational waves background as well as primordial black holes. These primordial black holes can interact among themselves, and other astrophysical black holes to create a secondary gravitational wave. We combine these gravitational wave backgrounds to obtain the cumulative background. We also show the dependence of this cumulative background on the temperature of the phase transition.

Keywords: gravitational waves, primordial black holes, first order phase transition
DOI: 10.31526/BSM-2023.25

1. INTRODUCTION

The nature of dark matter is arguably one of the most discussed topics in the current paradigm of particle physics and cosmology. Dark matter can be particulate in nature or some exotic compact object, such as primordial black holes (PBH). PBHs are hypothecized to be created in the very early universe by non-stellar means. Whether theoretically a large range of mass is possible for the PBH, various observational constraints restricts the parameter space over which PBHs can partially or fully play the role of dark matter in standard cosmology.

Though PBHs are thought to have been generated in the early epoch of the universe, throughout the evolution of the universe many mechanisms can give rise to PBHs, such as single or multi-field inflations, the collapse of cosmic strings, critical collapse, first-order phase transitions (FOPT), etc. Here we are interested in the FOPT as the origin of PBHs. FOPTs can occur in many beyond the standard model (BSM) scenarios, in some cases they can create PBHs. We consider the delayed decay of false vacuum as the method of PBH creation in a model-independent way [1, 2, 3, 4].

Along with PBHs, FOPTs are most popular source of the stochastic gravitational wave background (SGWB). Since we are moving into the era of gravitational wave astronomy thanks to the many proposed gravitational wave experiments such as LISA, DECIGO, BBO, ET, CE which will be running in the upcoming decades, we aim to use the cumulative gravitational wave background created directly and indirectly (i.e., through the interactions of the PBHs) by the FOPT to probe it as the origin of PBHs. It is worth mentioning here that, along with FOPT, all the other methods that can create PBH and SGWB can be probed similarly.

This article is organized as follows, in Section 2, we explain the mechanisms through which the PBHs and the SGWB are created due to the FOPT. In Sections 3 and 4, we focus on the creation of secondary SGWB from the interactions of the PBHs among themselves and the astrophysical black holes (ABH) respectively. The results are discussed in Section 5 and finally in Section 6, we summarize and conclude.

2. CREATION OF PBHS AND SGWB FROM FOPT

The ever-evolving universe has possibly gone through a few phase transitions during its lifetime. This can be materialised as the universe evolves and cools down, it might find that the minima it has been residing are not the true minima, i.e., there might originate a new *true* minima, and the minima the universe has been being termed as the *false* minima. The journey of the universe, by means of quantum tunnelling, from the false minima to the true minima, is called a *phase transition*. The nature of the phase transition depends on the potential driving this phase transition, i.e., if there is a barrier between these two minima that can only be crossed through tunnelling (quantum or thermal), then the transition is called a first-order phase transition. Otherwise, it can be a second-order phase transition. The first order phase transition is the one that we are interested in as it can create SGWB and PBHs. Although not in the SM, many well-motivated BSM scenarios can give rise to FOPTs.

The thermal or quantum tunnelling from false to true vacuum physically manifests as nucleation of true vacuum bubbles, which might grow and collide, eventually taking the entire universe from false to true vacuum, releasing a tremendous amount of energy as latent heat. The temperature at which a second minima exists, which eventually becomes the true minima, is called the critical temperature (T_C). This depends on the particular model which is giving rise to the FOPT. The temperature at which the probability of nucleation of one true vacuum bubble per Hubble volume is unity is called the nucleation temperature (T_N). The

probability of nucleation of bubble can be mathematically expressed as $\Gamma = \Gamma_0 e^{\beta(t-t_0)}$, where β can be expressed as

$$\beta = -\left.\frac{dS(t)}{dt}\right|_{t=t_0}, \tag{1}$$

where t_0 is an appropriate time around which the phase transition occurs, and $S(t)$ is the bounce action of the instanton solution. These bubbles nucleate and expand and eventually some of them collide with each other releasing a huge amount of energy as gravitational waves. These waves then evolve with the evolving universe creating a background, which is called the SGWB. The features of these SGWB depend upon the parameters of the FOPT, i.e. α which is a measure of the strength of the FOPT, β which is a measure of the time duration of the FOPT, κ which carries information regarding the fraction of the energy that is released to the plasma and T which is the transition temperature.

Apart from this, since the nucleation of the true vacuum bubbles is a probabilistic process, there is a finite probability that the nucleation of true vacuum bubbles is delayed in some Hubble regions. As a result, while the energy density of the regions that have already converted to a true vacuum dilutes, these regions that are in a false vacuum and thus dominated by vacuum energy maintain a constant energy density. After a while, when this vacuum energy is converted to radiation, these regions have an overdensity. If this overdensity exceeds a certain threshold, it collapses to form a PBH. As mentioned above, the mass and abundance also depend on the different FOPT parameters.

We now elaborate on both of these processes and we give the properties of these PBHs and SGWB for a few benchmark cases.

2.1. Creation of PBHs

As mentioned above, the creation and vital statistics of PBHs sensitively depend on the FOPT parameters. For example, for larger α values, the abundance of PBHs are larger. This is due to the fact that α signifies higher energy difference between the two vacuums and therefore, the overdensity would reach the threshold value sooner. On the contrary, larger β exponentially reduces the abundance of the PBHs. This is because larger β corresponds to a shorter duration for the FOPT, which also suggests that the phase transition reaches completion before the overdensity can reach the threshold for collapse. However, the exact dependence is quite involved, for detailed discussions see [1, 2, 3, 4]. The mass of the PBHs depends only on the transition temperature. We take this to be the nucleation temperature. However, model-dependent studies are required to obtain the exact temperature at which the overdense region reaches the threshold for collapse. It is assumed the entire Hubble sized overdense region collapses to for a PBH. Therefore, the PBH mass can be expressed as function of temperature such as

$$M = 1.45 \times 10^5 \left(\frac{g_*}{10.75}\right)^{-\frac{1}{2}} \left(\frac{T}{\text{MeV}}\right) M_\odot, \tag{2}$$

where T is the transition temperature.

We consider two benchmark cases shown in Table 1, among which the higher temperature one is motivated by a singlet scalar extension of standard model and the lower temperature can be motivated by dark sector scenarios. For these two benchmark scenarios we show the abundances of the PBH population in the left panel of Figure 1. It can be seen that the higher temperature FOPT gives rise to $3 \times 10^{-5} M_\odot$ PBHs with an abundance of 0.01 whereas the lower temperature PBH gives rise to $40 M_\odot$ PBHs with an abundance of 0.005. We also show the relevant constraints on the PBH abundances. It is to be noted here that the benchmark cases that we have taken are within the constraints obtained from different observations. It is to be noted here that model-dependent analysis is required to obtain the exact values of the FOPT parameters and thus the properties of the PBH population.

Parameters	I	II
T (in GeV)	0.06	45
α	1	1.5
β/H	3.5	2.5
κ	0.5	1

TABLE 1: The relevant parameters describing the different FOPTs.

2.2. Creation of GW

The creation of SGWB, as explained before are also a direct consequence of the FOPTs. There are a few different ways through which FOPTs can generate SGWBs and they are collision of bubbles, sound waves and the magnetohydrodynamic turbulence. Here we focus on the SGWB due to the bubble wall collisions to show the order of magnitude of the SGWBs created due to the benchmark cases we consider, however, this can easily be extended to the other mechanisms as well. The SGWB can be expressed as,

$$\Omega_{\text{GW}}(f) = 1.67 \times 10^{-5} \left(\frac{H}{\beta}\right)^2 \left(\frac{\kappa\alpha}{1+\alpha}\right)^2 \frac{0.11 v_w^2}{0.42 + v_w^3} \left(\frac{3.8\left(f/f_p\right)^{2.8}}{1 + 2.8\left(f/f_p\right)^{3.8}}\right), \tag{3}$$

where

$$f_p = \frac{0.62}{1.8 - 0.1v_w + v_w^2}\left(\frac{\beta}{H}\right)\frac{T}{100\,\text{GeV}}\left(\frac{g_*}{100}\right)^{1/6} \times 1.65 \times 10^{-5}\,\text{Hz} \tag{4}$$

is the peak frequency and v_w is the bubble wall velocity. As mentioned earlier, the SGWB also depends on the different FOPT parameters. In the right panel of Figure 1 we show the spectra of the SGWB created due to the two benchmark cases that we have considered in Table 1. It is worth mentioning here that detailed numerical analysis is required to obtain the bubble wall velocity, however since that is outside the scope of our study, we have taken the bubble wall velocity equal to the speed of light, i.e., $v_w \sim 1$.

Now that we have shown the direct consequences of the FOPT, i.e., the PBH population and the SGWB, we focus in the indirect ways, i.e., the secondary SGWB spectra generated out of the interactions between these PBHs among themselves and with other ABHs.

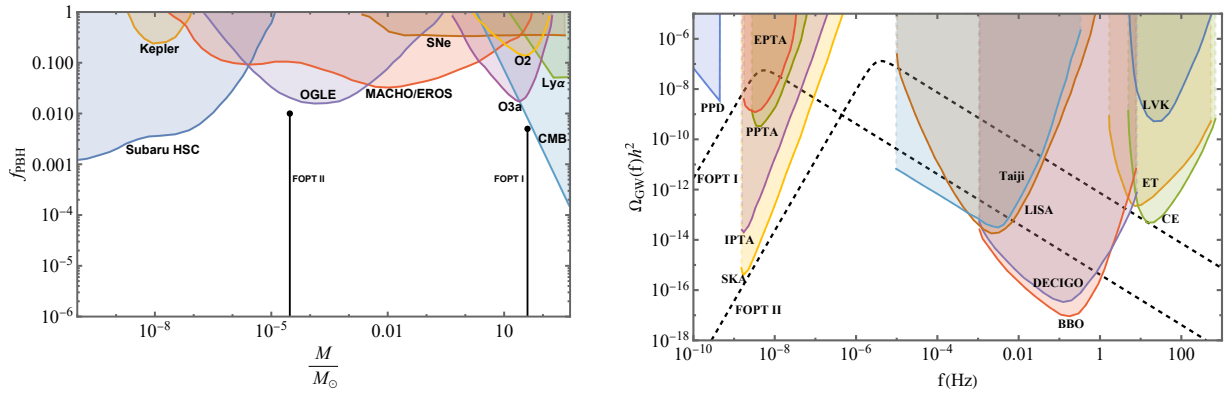

FIGURE 1: *Left*: abundances for different PBH masses. The constraints from Subaru HSC [5], Kepler [6], OGLE [7], MACHO/EROS [8, 9], SNe [10], Ly-α [11], CMB [12] and the non-observation of SGWB from the second observing run (O2) and the first half of the third observing run (O3a) of LVC [13] have also been shown. *Right*: the SGWB spectrum for the two first order phase transitions considered in this paper. The sensitivity curves for SKA [14], IPTA [15], EPTA [16], PPTA [17], Taiji [18], LISA [19], DECIGO [20], BBO [21], CE [22], ET [23], LIGO, Virgo and KAGRA (LVK) [24, 25] have been shown. The constraints from pulsar parameter drifts (PPD) [26] have also been shown.

3. PBH-PBH INTERACTIONS

The PBHs created due to the FOPTs can interact among themselves in different ways, i.e., two PBHs can come close to each other to form binary black holes (BBH) or they can go through individual scattering events, which are also known as close hyperbolic encounters (CHE). The BBHs can create different types of gravitational waves, e.g., (i) short-lived transient signals created by individual events, (ii) signals which last longer than observational period, and (iii) SGWB created by unresolvable binaries. Similarly, CHEs can also create transient signals or they can create SGWB. In this article we mainly focus on the SGWB created by BBH and CHE.

In the previous section, we describe how FOPTs can create SGWB; now we focus on how individual unresolvable events can source SGWB. In case of such a source we consider the individual events as point-like events and the spectrum of the gravitational waves can be expressed as

$$\Omega_{\rm GW}(f) = \frac{1}{\rho_c}\int_0^\infty dz \frac{N(z)}{1+z}\frac{dE_{\rm GW}}{d\ln f_s}, \tag{5}$$

where ρ_c is the critical density of the universe, z is the redshift, $f_s = (1+z)f$ is the GW frequency in the source frame, and $N(z)$ is the number density of the GW events at redshift z. This number density can be expressed as

$$N(z) = \frac{\tau(z)}{(1+z)H(z)}, \tag{6}$$

where $\tau(z)$, which has units of $\text{yr}^{-1}\,\text{Gpc}^{-3}$, is the number of events per unit time per unit comomving volume and $H(z)$ is the Hubble expansion coefficient. In case of PBH population with two different masses interacting with each other, the event rate can be expressed as

$$\tau(z) = \int\int \frac{dm_1}{m_1}\frac{dm_2}{m_2}\frac{d\tau}{d\ln m_1 d\ln m_2}. \tag{7}$$

For simplicity, we consider the number of events to be independent of the redshift. It is to be noted here that the event number τ or the energy released in the form of gravitational waves per logarithmic frequency bin $dE_{\rm GW}/d\ln f_s$ depends on the event type, i.e., whether they are BBH and CHE. We elaborate this in the following subsections.

3.1. PBH-PBH Binaries

Now we elaborate further on the PBH-PBH binary formation. Two PBHs, depending on their initial position and velocity, may come close to each other and form binary systems. This event happens in three different stages, i.e., inspiral, merger and ringdown. The energy released from the system per logarithmic frequency bin is different for these three different stages see [27] (and references therein) for further information. The number of events per logarithmic mass interval for PBH binary systems can be expressed as

$$\frac{d\tau_{\rm BBH}}{d\ln m_1 d\ln m_2} = 14.8\,{\rm yr}^{-1}\,{\rm Gpc}^{-3} f(m_1)\, f(m_2)\, \frac{M^{10/7}}{(m_1 m_2)^{5/7}} \left(\frac{\Omega_{\rm DM}}{0.25}\right)^2 \left(\frac{\delta_{\rm loc}}{10^8}\right) \left(\frac{v_0}{10\,{\rm km/s}}\right)^{-11/7}, \tag{8}$$

where $\Omega_{\rm DM}$ is the density parameter of the dark matter, the local density of the dark matter is expressed by $\delta_{\rm loc}$ and it can be taken to be $\mathcal{O}(10^8)$, v_0 signifies the initial velocity between two PBHs that create the binary system and eventually merge to form a bigger black hole, $M = (m_1 + m_2)$ is the total mass of the two black holes, $f(m_1)$ and $f(m_2)$ are the two logarithmic mass function which are defined such that, $\int f(m)/m dm = f_{\rm PBH}$. For simplicity, we consider the PBH populations to have monochromatic mass functions, i.e., all the PBHs formed during a particular FOPT are considered to have the same mass.

Considering these details of the PBH-PBH BBH systems and utilising equation (5), we obtain the SGWB spectrum due to the formation of the mergers between the PBHs. We show this in the left panel of Figure 2. For illustrative purposes we considered the interactions between two $40M_\odot$ PBHs, one $40M_\odot$ and one $3\times10^{-5}M_\odot$ PBH and two $3\times10^{-5}M_\odot$ PBHs. However, only the first two cases give rise to significant SGWB, while the third case generates negligible SGWB. This is due the fact that the energy released in the form of GW is sensitive to the PBH mass and abundance. Though the lighter PBHs in our case have marginally higher abundance, they are so significantly lighter than the $40M_\odot$ PBHs that their interactions releases negligible energy. Therefore, in the left panel of Figure 2, we only show the SGWB due to the mergers of $40M_\odot$ PBHs among themselves and with $3\times10^{-5}M_\odot$ PBHs. It can be seen that only the merger between the $40M_\odot$ creates SGWB which is within the sensitivity range of BBO.

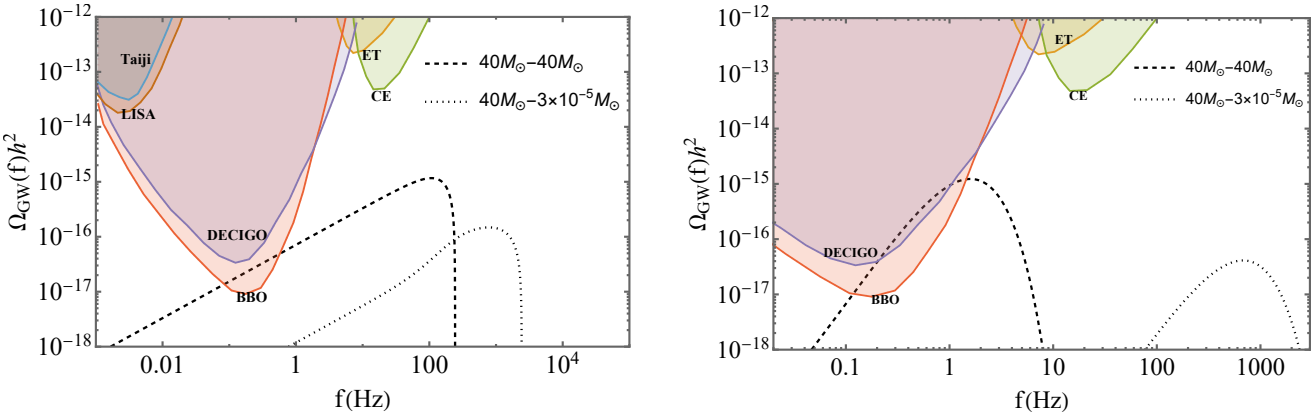

FIGURE 2: *Left*: the SGWB spectrum for PBH binaries of mass combinations $40M_\odot - 40M_\odot$ and $40M_\odot - 3\times10^{-5}M_\odot$. The relevant sensitivity curves have been shown. *Right*: the SGWB spectrum for PBH CHE of mass combinations $40M_\odot - 40M_\odot$ and $40M_\odot - 3\times10^{-5}M_\odot$. The relevant sensitivity curves have been shown.

3.2. Close Hyperbolic Encounters of PBH

Now we shift our focus to close hyperbolic encounters of PBH. Unlike the previous case, two PBHs can approach each other and scatter off of each other releasing some energy in the form of gravitational waves. This is called close hyperbolic encounters of PBHs. The event rate in this case can be expressed as

$$\frac{d\tau_{\rm CHE}}{d\ln m_1 d\ln m_2} = 25.4\times10^{-8} \left(\frac{\Omega_{\rm DM}}{0.25}\right)^2 \left(\frac{\delta_{\rm loc}}{10^8}\right) f(m_1)\, f(m_2)\, \frac{M^2}{m_1 m_2} \frac{e^2-1}{(v_0/c)^3}, \tag{9}$$

where e is the eccentricity of the path taken by the PBHs. The energy per logarithmic frequency interval in this case is different than the previous case and depends heavily on the geometry of the path taken by the PBHs see [27] and references therein.

Plugging these considerations in equation (5) we obtain the SGWB spectrum due to the CHEs of PBHs. Like the previous case, here also we obtain it for all the three combination of PBH masses, however, only the first two combinations give significant contributions which we have shown in the right panel of Figure 2. It can be seen that like the previous case, here also, only close hyperbolic encounters of $40M_\odot$ creates detectable SGWB within the sensitivity range of both BBO and DECIGO. In order to generate the SGWB spectrum for the PBH-PBH CHE, we have taken a few benchmark parameters regarding the geometry of the path taken by the PBHs and for further information regarding these, we encourage the reader to see [27].

4. PBH-ABH INTERACTIONS

Apart from the interaction between themselves, PBHs can also interact with other ABHs. However, in this case we have to take in to account that unlike the PBHs, which were formed in very early universe, i.e., at very high redshift, ABHs were formed fairly recently. Therefore, while considering the interactions between PBH and ABH, we have to modify the equation (5), i.e., in the upper limit of the interaction we put 5 instead of ∞. It is also to be noted that calculating the ABH population is far more complicated than than the previous case. However, for our purpose, we use a rough estimate, i.e., there are 2×10^{-3} ABHs in every one solar mass of galactic matter in the universe. We also consider the ABH masses to be between 5 and a few tens of solar masses. There are a few more details which are different in this case than the case of PBH-PBH interactions, for which we direct the readers to [27] (and references therein).

Taking these considerations we obtain the SGWB for PBH-ABH binary systems and we show them in the left panel of Figure 3. It can be seen that the SGWB due to the binaries of ABH and PBH of masses $40M_\odot$ is non-negligible, i.e., it is within the sensitivity curve of BBO, however for the PBHs of mass $3 \times 10^{-5} M_\odot$ the SGWB is not detectable by any current or proposed GW observatories.

Similarly, we show the SGWB due to the CHE between PBH and ABH as well in the right panel of Figure 3. Like the case of PBH-ABH BBH, in this case as well, the SGWB due to the heavier PBHs are much more significant than the lighter ones, but yet they are only marginally within the sensitivity range of BBO.

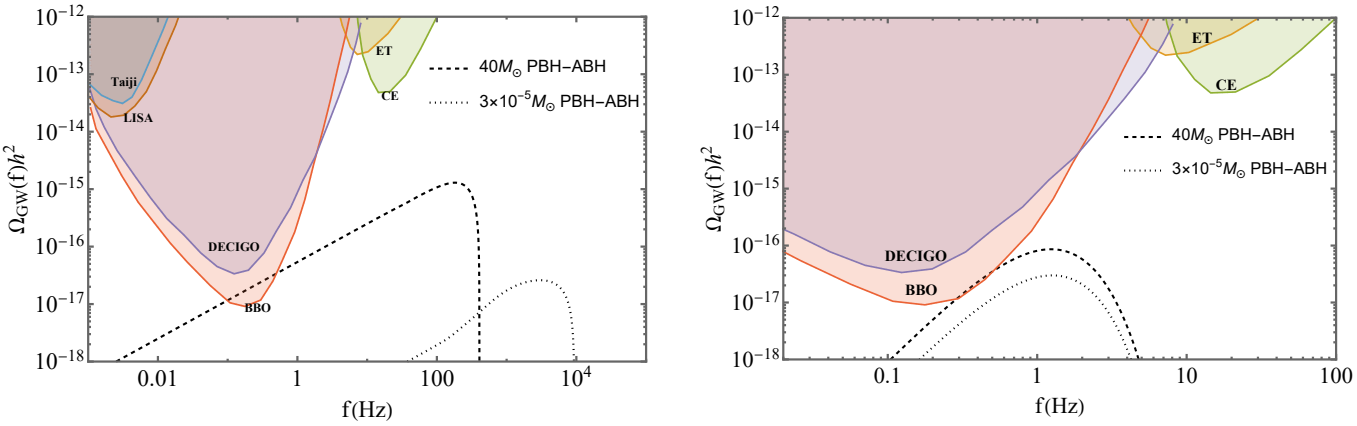

FIGURE 3: *Left*: the SGWB spectrum for PBH-ABH binaries for PBH mass $40M_\odot$ and $3 \times 10^{-5} M_\odot$. The relevant sensitivity curves have been shown. *Right*: the SGWB spectrum for PBH-ABH CHE for PBH mass 40 $M_\odot$ and $3 \times 10^{-5} M_\odot$. The relevant sensitivity curves have been shown.

5. RESULTS

Now we focus on the results which are divided in three main parts, i.e., (i) the cumulative background gravitational waves which was the main aim of this article, (ii) the peak frequencies of the different part of the cumulative background which gives us an idea regarding the detectability of the entire cumulative background and (iii) the dependence of the cumulative background on the FOPT temperature.

5.1. Cumulative Background

One of the main aims of this article was to obtain the cumulative background gravitational waves due to a FOPT. This cumulative background consists of two parts, (i) the SGWB generated directly from the FOPT (primary SGWB) and (ii) the SGWB which is the indirect consequence of the FOPT (secondary SGWB). The first one is generated from the collision of bubble walls during a FOPT, however the second one is created from the interaction of the PBHs which were created during the FOPT amongst themselves and other ABHs.

Now in order to show all of them together for a particular FOPT, we consider the the low temperature benchmark, i.e., the FOPT at 60 MeV and we show the result in Figure 4. It can be seen that the primary SGWB is the highest in magnitude, which is within the sensitivity range of PTAs, Taiji, LISA, DECIGO, and BBO. Among the components which create the secondary SGWB, the ones which are due to PBH-PBH interactions are higher in magnitude than the ones created due to PBH-ABH interactions for most of the frequency range. For even lower temperature FOPTs, i.e., for higher mass PBHs, the SGWB due to the PBH-PBH interactions will overshadow the ones due to the PBH-ABH interactions even more. However, for the FOPTs at temperature higher than a few GeVs, the SGWB due to the PBH-ABH interactions would dominate. It can also be seen from Figure 4 that as opposed to just the primary SGWB, the cumulative SGWB has more features towards the tail, which, if present (absent) along with the primary SGWB can be used to favour (refute) FOPT as the the creation mechanism of the PBHs. However, it must be taken into account that, most of the tail, for FOPTs around or above $\mathcal{O}(100)$ MeV will be undetectable with the proposed GW experiments.

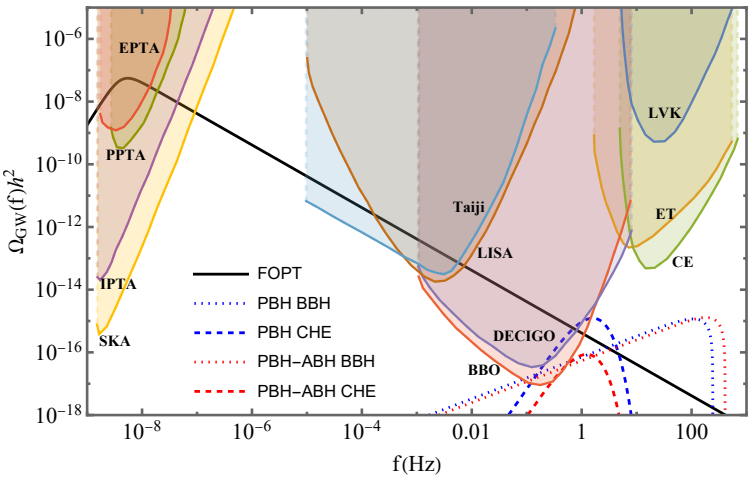

FIGURE 4: The SGWB spectra originating from different processes for FOPT at $T = 60\,\text{MeV}$ which corresponds to the PBHs of mass $40M_\odot$.

Since this cumulative SGWB has many features, we now shift our focus to the peaks of the different parts of the SGWB. The first one is straight forward, as the peak frequency of the SGWB due to the FOPT is mentioned in equation (4). The peaks of the secondary SGWB can be divided in two different parts, i.e., the one for the peak due to the binary and the oner for the CHE. The peak due to the BBH can be expressed as

$$f_{\text{peak}}^{\text{BBH}} = 0.12 \left(\frac{g_*}{10.75}\right)^{1/2} \left(\frac{T}{\text{MeV}}\right) \text{Hz}, \tag{10}$$

and the peak frequency due to the CHE is

$$f_{\text{peak}}^{\text{CHE}} = 46 \left(\frac{g_*}{10.75}\right)^{-1/4} \left(\frac{T}{\text{MeV}}\right) \text{Hz}. \tag{11}$$

As it can be seen, all three of these peak frequencies depend on the transition temperature. This is due to the fact that the peak frequencies of the primary, i.e., the SGWB due to FOPT depends on the Hubble volume at the time of its creation which in turn depends on the temperature of the universe, and the secondary, i.e., the SGWB due to the interactions of the PBH depend on the PBH mass, which as mentioned earlier, depends on the FOPT temperature. It is worth mentioning here that for the two different peaks of the secondary SGWB, we have only considered the PBH-PBH interactions as they are more dominant in the parameter domain that we consider. In Figure 5, we elaborate this behaviour even further.

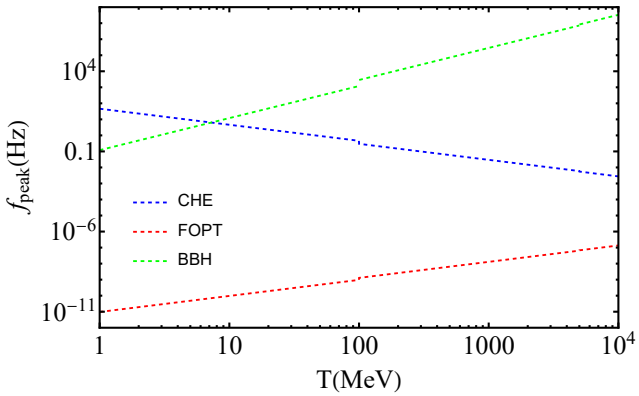

FIGURE 5: The dependences of the peak frequencies of the SGWB spectrum originating from different sources on the temperature of the FOPT.

As it can be seen from Figure 5, in the frequency range between 100 to 1000 MeV, all three of the peak frequencies are within the sensitivity range of the current and the future GW experiments. However, above that temperature thought the peak due to FOPT and CHE are within the sensitivity range of the different GW experiments, the peak due to the BBH is above the range of the interferometer experiments. It also to be noted that below 100 MeV, the peak due to the FOPT is outside of the sensitivity range of the PTAs, however, most of the primary spectra can still be probed using the PTAs and the different interferometer experiments.

Now we move to the dependence of the cumulative SGWB on the transition temperature of the FOPT. In order to show that, we consider three FOPTs at temperatures 16 MeV, 60 MeV, and 200 MeV. We show the cumulative SGWB for these three cases in Figure 6.

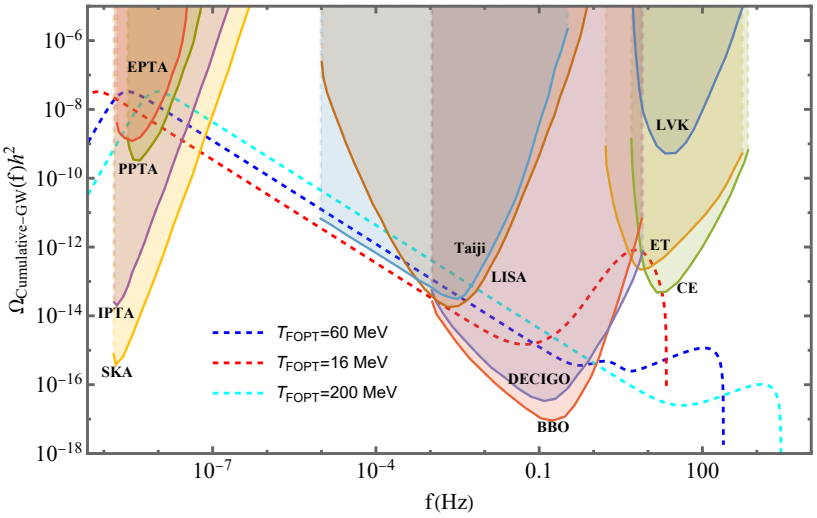

FIGURE 6: The cumulative SGWB spectra originating due to FOPTs at different temperatures.

It can be seen that if all other variables, i.e., α, β/H are kept constant, the peak of primary shift towards the higher frequency with the increasing temperature but the magnitude remains almost the same. This is due to the fact that the magnitude of the primary SGWB depend on the FOPT parameters other than the transition temperature. However, as mentioned earlier, the abundance of the PBH population is extremely sensitive to α and β/H. But since we are focussing on the effect of the transition temperature on the cumulative background, we consider the benchmark value of the abundance to be 0.005 in all the cases. In that case, we can see that the tail of the cumulative SGWB increases in magnitude as the temperature of the FOPT decreases. The reason behind this is as the temperature of the FOPT decreases the mass of the PBH increases and the secondary SGWB, i.e., the SGWB due to the PBH-PBH interactions increase in magnitude as the PBH masses increase. It is to be kept in mind that in realistic scenarios, a specific model has to be chosen and the entire analysis has to be performed to obtain the FOPT parameters and the properties of the PBH population to obtain the cumulative background which is beyond the scope of the current study.

6. CONCLUSION

In this article we consider the cumulative SGWB created during a FOPT to probe the creation of PBHs during that FOPT. The cumulative background consists of the primary SGWB, which is created due to the FOPT and the secondary background which is generated by the interactions of the PBHs which are also created during the FOPT. Though there are a few proposed mechanism through which PBHs can be created during a first order phase transition, in this article we consider the delayed decay of false vacuum during FOPT as the creation mechanism for PBHs. It is to be mentioned here, that the primary SGWB, i.e., the SGWB due to the FOPT can be created in a few different ways, however we just take into account the collision of true vacuum bubbles in this case.

We first consider two benchmark cases and show the PBH population and the SGWB spectra due to these two cases. The SGWB due to the FOPT is considered as the primary SGWB spectra. Next we consider the PBHs and we obtain the SGWB spectra due to the interactions of these PBHs among themselves and with other ABHs. We consider two different interactions, namely, (i) creation of PBH-PBH or PBH-ABH binary systems and (ii) single scattering events between two PBHs or one PBH and one ABH which are also known as close hyperbolic encounters. In the first case, two black holes come close two each other and creates a bound system and eventually merge with each other releasing a large amount of energy in the form of gravitational waves. In the second one two black holes come close to each other but due to the geometry the path, they do not form a bound system, but they also release energy in the form of gravitational waves. In this study we consider the portion these events which are unresolvable and thus creates SGWB. Since this is also an indirect consequence of the FOPT, we call this the secondary SGWB spectra. Considering the two of them together we obtain the cumulative SGWB spectra. This cumulative spectra consist of a larger low frequency peak, i.e., the primary SGWB and one or more smaller high frequency secondary peaks. For one of our benchmark case, i.e., the benchmark case where the FOPT temperature is 60 MeV (which creates $40M_\odot$ PBHs), we see that though the secondary peaks due to the PBH-PBH interaction dominates, it can only be probed in futuristic detectors such as BBO or DECIGO. We show that the cumulative spectra has features which can be used to gain information regarding the origin of the PBH population. We further show the dependence of the different peaks of the cumulative spectra on the transition temperature. Finally we present the dependence of this cumulative spectra on the FOPT temperature. We see that when all the other parameters such as α, β/H, and $f_{\rm PBH}$ are kept fixed, with the temperature of the FOPT the magnitude of the secondary peaks are enlarged.

Finally we mention that though we have considered benchmark cases in our work, model dependent studies are required to obtain the FOPT parameters and the PBH population to evaluate the shape of the cumulative background. It is also worth mentioning that any mechanism, which can create both PBH and SGWB can be treated in a similar manner and a cumulative SGWB can be obtained.

References

[1] K. Kawana, T. Kim and P. Lu, *PBH Formation from Overdensities in Delayed Vacuum Transitions*, 2212.14037.
[2] J. Liu, L. Bian, R.-G. Cai, Z.-K. Guo and S.-J. Wang, *Primordial black hole production during first-order phase transitions*, *Phys. Rev. D* **105** (2022) L021303 [2106.05637].
[3] Y. Gouttenoire and T. Volansky, *Primordial Black Holes from Supercooled Phase Transitions*, 2305.04942.
[4] M. Lewicki, P. Toczek and V. Vaskonen, *Primordial black holes from strong first-order phase transitions*, 2305.04924.
[5] H. Niikura et al., *Microlensing constraints on primordial black holes with Subaru/HSC Andromeda observations*, *Nature Astron.* **3** (2019) 524 [1701.02151].
[6] K. Griest, A. M. Cieplak and M. J. Lehner, *New Limits on Primordial Black Hole Dark Matter from an Analysis of Kepler Source Microlensing Data*, *Phys. Rev. Lett.* **111** (2013) 181302.
[7] H. Niikura, M. Takada, S. Yokoyama, T. Sumi and S. Masaki, *Constraints on Earth-mass primordial black holes from OGLE 5-year microlensing events*, *Phys. Rev. D* **99** (2019) 083503 [1901.07120].
[8] MACHO collaboration, *MACHO project limits on black hole dark matter in the 1–30 solar mass range*, *Astrophys. J. Lett.* **550** (2001) L169 [astro-ph/0011506].
[9] EROS-2 collaboration, *Limits on the Macho Content of the Galactic Halo from the EROS-2 Survey of the Magellanic Clouds*, *Astron. Astrophys.* **469** (2007) 387 [astro-ph/0607207].
[10] M. Zumalacarregui and U. Seljak, *Limits on stellar-mass compact objects as dark matter from gravitational lensing of type Ia supernovae*, *Phys. Rev. Lett.* **121** (2018) 141101 [1712.02240].
[11] R. Murgia, G. Scelfo, M. Viel and A. Raccanelli, *Lyman-α Forest Constraints on Primordial Black Holes as Dark Matter*, *Phys. Rev. Lett.* **123** (2019) 071102 [1903.10509].
[12] V. Poulin, P. D. Serpico, F. Calore, S. Clesse and K. Kohri, *CMB bounds on disk-accreting massive primordial black holes*, *Phys. Rev. D* **96** (2017) 083524 [1707.04206].
[13] G. Hütsi, M. Raidal, V. Vaskonen and H. Veermäe, *Two populations of LIGO-Virgo black holes*, *JCAP* **03** (2021) 068 [2012.02786].
[14] C. L. Carilli and S. Rawlings, *Science with the Square Kilometer Array: Motivation, key science projects, standards and assumptions*, *New Astron. Rev.* **48** (2004) 979 [astro-ph/0409274].
[15] G. Hobbs et al., *The international pulsar timing array project: using pulsars as a gravitational wave detector*, *Class. Quant. Grav.* **27** (2010) 084013 [0911.5206].
[16] L. Lentati et al., *European Pulsar Timing Array Limits On An Isotropic Stochastic Gravitational-Wave Background*, *Mon. Not. Roy. Astron. Soc.* **453** (2015) 2576 [1504.03692].
[17] R. M. Shannon et al., *Gravitational waves from binary supermassive black holes missing in pulsar observations*, *Science* **349** (2015) 1522 [1509.07320].
[18] W.-H. Ruan, Z.-K. Guo, R.-G. Cai and Y.-Z. Zhang, *Taiji program: Gravitational-wave sources*, *Int. J. Mod. Phys. A* **35** (2020) 2050075 [1807.09495].
[19] LISA collaboration, *Laser Interferometer Space Antenna*, 1702.00786.
[20] S. Kawamura et al., *The Japanese space gravitational wave antenna: DECIGO*, *Class. Quant. Grav.* **28** (2011) 094011.
[21] S. P. et al., *The Big Bang Observer: Direct detection of gravitational waves from the birth of the Universe to the Present*, *NASA Mission Concept Study* (2004) .
[22] D. Reitze et al., *Cosmic Explorer: The U.S. Contribution to Gravitational-Wave Astronomy beyond LIGO*, *Bull. Am. Astron. Soc.* **51** (2019) 035 [1907.04833].
[23] M. Punturo et al., *The Einstein Telescope: A third-generation gravitational wave observatory*, *Class. Quant. Grav.* **27** (2010) 194002.
[24] KAGRA collaboration, *Detector configuration of KAGRA: The Japanese cryogenic gravitational-wave detector*, *Class. Quant. Grav.* **29** (2012) 124007 [1111.7185].
[25] LIGO Scientific collaboration, *Advanced LIGO*, *Class. Quant. Grav.* **32** (2015) 074001 [1411.4547].
[26] W. DeRocco and J. A. Dror, *Searching For Stochastic Gravitational Waves Below a Nanohertz*, 2304.13042.
[27] I. K. Banerjee and U. K. Dey, *Probing the origin of primordial black holes through novel gravitational wave spectrum*, *JCAP* **07** (2023) 024 [2305.07569].